Since January 2020 Elsevier has created a COVID-19 resource centre with free information in English and Mandarin on the novel coronavirus COVID-19. The COVID-19 resource centre is hosted on Elsevier Connect, the company's public news and information website.

Elsevier hereby grants permission to make all its COVID-19-related research that is available on the COVID-19 resource centre - including this research content - immediately available in PubMed Central and other publicly funded repositories, such as the WHO COVID database with rights for unrestricted research re-use and analyses in any form or by any means with acknowledgement of the original source. These permissions are granted for free by Elsevier for as long as the COVID-19 resource centre remains active.

Virology **278,** 75–85 (2000)
doi:10.1006/viro.2000.0637, available online at http://www.idealibrary.com on IDEAL®

Identification of a Noncanonical Signal for Transcription of a Novel Subgenomic mRNA of Mouse Hepatitis Virus: Implication for the Mechanism of Coronavirus RNA Transcription

Xuming Zhang[1] and Runzhong Liu

Department of Microbiology and Immunology, University of Arkansas for Medical Sciences, Little Rock, Arkansas 72205-7199

Recieved July 5, 2000; returned to author for revision August 21, 2000; accepted September 8, 2000; published online November 8, 2000

Subgenomic RNA transcription of coronaviruses involves the interaction between the leader (or antileader) and the intergenic (IG) sequences. However, it is not clear how these two sequences interact with each other. In this report, a previously unrecognized minor species of subgenomic mRNA, termed mRNA5–1, was identified in cells infected with mouse hepatitis virus (MHV) strains JHM2c, JHM(2), JHM(3), A59, and MHV-1. Sequence analysis revealed that the leader-body fusion site of the mRNA is located at approximately 150 nucleotides (nt) downstream of the consensus IG sequence for mRNA 5 and did not have sequence homology with any known IG consensus sequences. To determine whether this sequence functions independently as a promoter, we cloned a 140-nt sequence (from ≈70 nt upstream to ≈70 nt downstream of the fusion site) from viral genomic RNA and placed it in front of a reporter gene in the defective-interfering (DI) RNA-chloramphenicol acetyltransferase (CAT) reporter vector. Transfection of the reporter RNA into MHV-infected cells resulted in synthesis of a CAT-specific subgenomic mRNA detected by reverse transcription-polymerase chain reaction (RT-PCR). The strength of this promoter was similar to that of the IG7 (for mRNA 7) as measured by the CAT activity. Deletion analysis showed that the sequence as few as 13 nt was sufficient to initiate mRNA transcription, while mutations within the 13-nt abolished mRNA transcription. *In vitro* translation study confirmed that the envelope (E) protein was translated from mRNA5–1, which encodes the open reading frame (ORF) 5b at its 5′-end, indicating that mRNA5–1 is a functional message. Furthermore, when the ORF5b was replaced with the CAT gene and placed in the DI in the context of viral mini-genome, CAT was expressed not only from the first ORF of mRNA5–1 but also from the second and third ORF of mRNA5 and genomic DI RNA, respectively, suggesting that more than one mechanism is involved in regulation of ORF5b expression. Our findings thus support the notion that base-pairing between the leader (or antileader) and the IG is not the sole mechanism in subgenomic RNA transcription. © 2000 Academic Press

INTRODUCTION

Mouse hepatitis virus (MHV), a prototype of murine coronavirus, contains a single-strand, positive-sense RNA genome of ≈32 kb in length (Lee *et al.,* 1991; Pachuk *et al.,* 1989). Upon virus infection into susceptible cells, the viral genomic RNA serves both as an mRNA for translation of the putative RNA-dependent RNA polymerase polyprotein, which is required for subsequent RNA transcription and replication, and as a template for the synthesis of the genome-length, negative-strand RNA that in turn is used for the synthesis of the viral genome. Six to seven subgenomic mRNAs (mRNAs 2 to 7) are found in MHV-infected cells (Lai *et al.,* 1981; Leibowitz *et al.,* 1981). They are co-nested at the 3′-ends (Lai *et al.,* 1981; Leibowitz *et al.,* 1981). Each mRNA contains a leader sequence of approximately 70 nucleotides (nt) at the 5′-end, which is identical to the leader sequence of the genomic RNA (Lai *et al.,* 1983, 1984; Spaan *et al.,* 1983). Depending on MHV strains, there are two to four consensus UCUAA repeats with the last repeat being UCUAAAC, at the 3′-end of the leader (Makino and Lai, 1989a,b). An identical or similar consensus sequence is present between each gene, termed intergenic (IG) sequence (Budzilowicz *et al.,* 1985; Shieh *et al.,* 1989), which serves as a transcription initiation signal (promoter) for subgenomic mRNA synthesis (based on the leader-primed transcription model) or a termination signal for subgenomic negative-strand RNA synthesis (based on the discontinuous transcription on the negative-strand RNA) (Lai and Cavanagh, 1997, and references therein). The IG is the *cis*-acting sequence absolutely required for subgenomic RNA transcription (Makino *et al.,* 1991); it serves as a joining point between the leader (or antileader) and the remaining body part of each subgenomic RNA. For simplicity and consistency, we use the terminology according to the leader-primed transcription model (Lai and Cavanagh, 1997) throughout this report.

Direct sequencing of viral mRNAs have revealed varying numbers of UCUAA repeats at the 3′-end of the leader among certain subgenomic mRNA species of

[1] To whom reprint requests should be addressed at Department of Microbiology and Immunology, University of Arkansas for Medical Sciences, 4301 W. Markham St., Slot 511, Little Rock, AR 72205. Telephone: (501) 686-7415. Fax: (501) 686-5359. E-mail: zhangxuming@exchange.uams.edu

0042-6822/00 $35.00
Copyright © 2000 by Academic Press
All rights of reproduction in any form reserved.

JHM and JHM2c (Makino *et al.,* 1988, 1989a,b), the latter of which is a naturally occurring small plaque mutant of JHM (Makino *et al.,* 1984). Further sequencing on cDNA clones derived from JHM2c mRNAs by reserve transcription-polymerase chain reaction (RT-PCR) has shown that the leader-body joining sites in subgenomic mRNA2–1 are more heterogeneous (Zhang and Lai, 1994). In addition to the varying numbers of repeats, the joining sites of some mRNAs are located either upstream or downstream of the authentic consensus IG sequence, and they appear to be randomly distributed. The degree of such heterogeneity varies among JHM strains and mRNA species. Such phenomenon has also been observed in a recombinant MHV A59 expressing a green fluorescence protein (Fischer *et al.,* 1997). Two mRNA species smaller than mRNA7 were also identified in MHV-infected cells; they initiate from IG-like sequences UCCAAAC and UCUAAAU, respectively, within the nucleocapsid gene (Schaad and Baric, 1993). Thus, heterogeneity of leader-body joining sites in subgenomic mRNAs may be a common phenomenon for MHV.

The genomic and subgenomic mRNAs of coronaviruses are capped and contain multiple open reading frames (ORFs). In general, only the 5′-most ORF of each mRNA is translated into a protein via the cap-dependent ribosomal scanning mechanism, while the downstream ORFs are not translatable (Lai and Cavanagh, 1997, and references therein). An exception was found with the ORF5b of MHV, which encodes the E (envelope) protein. The E is a structural protein (Yu *et al.,* 1994) and is essential for virion assembly (Vennema *et al.,* 1996). It was found to be translated from the second ORF of the bicistronic mRNA5 *in vitro* (Thiel and Siddell, 1994, 1995), suggesting that translation of the E protein is cap-independent, possibly via an internal ribosomal entry site (IRES). Subsequently, the IRES has been roughly mapped through a series of deletion mutants to be located approximately between 100-nt upstream and 180-nt downstream of initiation codon for ORF5b (Jendrach *et al.,* 1999). The counterparts of the E gene in other coronaviruses include ORF5b of bovine coronavirus (BCoV), ORF4 of transmissible gastroenteritis virus (TGEV) and human coronavirus (HCoV) 229E, and ORF3c of avian infectious bronchitis virus (IBV) (Godet *et al.,* 1992; Smith *et al.,* 1990; Siddell, 1995). Interestingly, while ORF5b of BCoV and ORF4 of TGEV and HCoV are translated from the first ORF of mRNA5–1 and mRNA4, respectively, the ORF3c of IBV and ORF5b of MHV are translated from the third and second ORF of mRNA3 and mRNA5, respectively. More intriguingly, within TGEV strains, the ORF3b of Muller strain is translated from the second ORF of mRNA3 via an IRES, whereas that of the Purdue strain is translated from the first ORF of mRNA3–1 via cap-dependent mechanism (O'Connor and Brian, 2000). It is not known, however, why strains of the same TGEV or of various coronaviruses evolved such distinct mechanisms in regulation of their gene expression.

During the course of studying MHV transcriptional regulation, we unexpectedly identified a minor species of subgenomic mRNA in JHM2c-infected cells. Subsequently, the same mRNA species was identified in other MHV strains. We found that the leader-body joining site for this mRNA is located approximately 150-nt downstream rather than the authentic consensus IG sequence for mRNA5. We thus named mRNA5–1 for this novel mRNA species, and accordingly, IG5–1 for this transcription initiation site. When it was placed in front of the chloramphenicol acetyl-transferase (CAT) gene in the defective-interfering (DI) RNA-CAT reporter plasmid, the IG5–1, which is devoid of any known IRES sequence, can direct the synthesis of a subgenomic CAT-containing mRNA and expression of the CAT activity, thus confirming that the IG5–1 serves as a promoter for transcription of a subgenomic mRNA. Deletion analyses identified that a 13-nt sequence is sufficient for driving the reporter gene transcription. Furthermore, *in vitro* translation study confirmed that the E protein is translated from mRNA5–1, suggesting that mRNA5–1 is likely a functional message in virus-infected cells.

RESULTS

Heterogeneity of mRNA5 transcripts of MHV JHM2c in infected cells. Previous studies have shown that subgenomic mRNA2–1 of a small plaque mutant JHM2c is more heterogeneous in the leader-body joining site than that of its parental JHM strain, and that, even within the same JHM2c strain, mRNA2–1 is more heterogeneous than mRNA7 (Zhang and Lai, 1994). To understand whether such heterogeneity is virus-strain specific or mRNA-species specific, we have undertaken systematic analyses on the structure of all subgenomic mRNA species of JHM2c. DBT cells were infected with JHM2c at a multiplicity of infection (m.o.i.) of 5 in the presence of actinomycin D. Intracellular RNAs were extracted from infected cells at 8 h postinfection (p.i.). cDNAs were amplified by reverse transcription-polymerase chain action (RT-PCR) with a sense primer specific to the leader sequence and an antisense primer specific to a sequence downstream of the IG for each subgenomic mRNA. PCR products were directly cloned into the pTOPO2.1 TA vector. Inserts were then released from the vector by digestion with a restriction endonuclease *Eco*RI and were analyzed by agarose gel electrophoresis. We found that heterogeneity of subgenomic mRNAs occurred in all mRNA species (Fig. 1, and further data not shown). While it was consistent with the previous finding that the heterogeneity at the leader-body fusion site appeared to be randomly distributed (Zhang and Lai, 1994), transcripts amplified from mRNA5-specific primers exhibited another distinct subset. As shown in Fig. 1B,

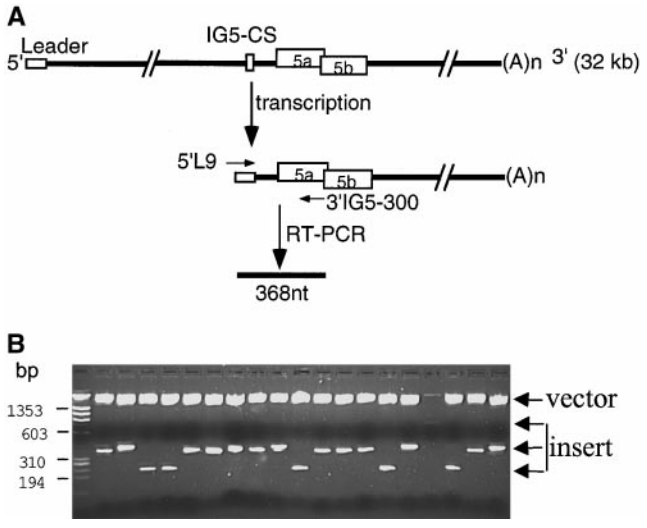

FIG. 1. Heterogeneity of subgenomic mRNA 5 of MHV JHM2c. (A) Schematic diagram depicting the structure of the genome and subgenomic mRNA5. IG5-CS, intergenic consensus sequence for transcription of mRNA5. The two primers used for RT-PCR and the predicted size of the PCR products are shown. 5a and 5b, open reading frame 5a and 5b. Leader, leader RNA. (B) Results of agarose gel electrophoresis analysis. PCR products from (A) were cloned into the pTOPO2.1 TA cloning vector. Plasmid DNAs were isolated from individual colonies, digested with *Eco*RI (two *Eco*RI sites franking the cloning site of the vector), and analyzed by electrophoresis on a 2% agarose gel. Arrows indicate the vector and the released inserts. Molecular weight marker in base pair (bp) is shown on the left.

three types of cDNA inserts for mRNA5 were identified. Fourteen of the 20 clones analyzed had a size corresponding to mRNAs initiating at the authentic consensus IG5 site. One had a size larger than the authentic mRNA5. Surprisingly, a quarter (5/20) of clones had a size smaller than the authentic mRNA5, suggesting that these transcripts possibly initiated at a downstream sequence. These results indicate that mRNA 5 of JHM2c is also heterogeneous, but that a second initiation site might be present at a downstream location.

A noncanonical sequence downstream of the consensus intergenic sequence for mRNA5 likely serves as a leader-body fusion site for a smaller species of subgenomic mRNA. To confirm that the cDNA clones shown in Fig. 1 indeed represent mRNA5, and if so, what are the structural feature of these clones at the leader-body joining sites, all 20 clones were sequenced with an automated DNA sequencer. As shown in Fig. 2A, all 20 clones contained sequences corresponding to mRNA5 of JHM2c, indicating the specificity of the RT-PCR products. Consistent with the data from agarose gel analysis (Fig. 1), the leaders of the 14 clones fused to the body at the authentic consensus IG sequence (UCUAAAC) (Fig. 2A). In one clone, the leader fused to a sequence upstream of the consensus IG sequence. This clone was not pursued for further experiments due to its singularity. All the other five smaller clones had a leader fused to a nonconsensus sequence approximately 150-nt downstream of the authentic consensus IG sequence, with only three nucleotides complementary to the template (Figs. 2A and 2B). These sequence data indicate that the noncanonical downstream sequence possibly serves as a site for leader-fusion for a smaller subgenomic mRNA species, which is termed mRNA5–1.

To further determine whether mRNA5–1 is transcribed also in other MHV strains, DBT cells were infected with JHM(2), JHM(3), A59, and MHV-1 at m.o.i. of 5. Intracellular viral RNAs were isolated. The primer pair 5′-L9 and 3′-IG6–50 was used for amplifying the 5′-end of mRNA5–1 in RT-PCR. Two rounds of PCR for a total of 65 cycles were performed. The PCR fragments of ≈600 nt in length were gel-purified and used for direct sequencing. As shown in Figs. 2C–2F, the DNA fragments of the four MHV strains contain the same leader-body junction site that is identical to that of the IG5–1 of JHM2c (see Fig. 2B). These results thus confirm the existence of mRNA5–1 in all five MHV strains studied that uses the downstream IG5–1 sequence as the leader-fusion site. It is worth noting that minor species of mRNAs other than mRNA5–1 might exist, which could not be identified by direct sequencing of PCR fragments.

The noncanonical transcriptional signal is a functional promoter for the synthesis of a subgenomic mRNA in a DI RNA-CAT reporter system. To test whether this noncanonical sequence can serve as a transcription initiation site (promoter) for a reporter gene, a sequence of 140-nt encompassing approximately 70 nt each of the upstream and downstream of the leader-fusion site was placed in front of a CAT reporter gene in a DI RNA vector (Liao and Lai, 1994; Zhang *et al.,* 1994). The DI RNA-CAT reporter system has been extensively used for studying MHV replication, transcription, and gene expression (Liao and Lai, 1994; Liao *et al.,* 1995; Zhang and Lai, 1994; Zhang *et al.,* 1994, 1997, 1998). If the noncanonical signal serves as a promoter, a CAT-containing subgenomic mRNA would be transcribed in helper MHV-infected cells and the CAT activity would be expressed. As shown in Fig. 3A, the CAT activity expressed from DECAT5–1-transfected cells was as high as that from DECAT7, which contains the promoter sequence for transcription of mRNA 7 (Zhang *et al.,* 1994). This result indicates that the 140-nt noncanonical sequence drives the expression of the CAT gene in the DI RNA reporter plasmid.

Because it is reported that MHV ORF5b is translated from mRNA5 via an IRES sequence (Thiel and Siddell, 1994, 1995), it is important to determine whether the CAT activity resulted from translation of the bicistronic DI RNA or of a separate subgenomic mRNA, even though this 140-nt sequence does not contain the IRES sequence recently identified by Jendrach *et al.* (1999). To directly identify the CAT-containing subgenomic mRNAs, RNAs were isolated from MHV-infected and DECAT5–1 RNA-transfected cells. RNAs isolated from DECAT7 RNA-transfected cells and from mock-transfected cells were

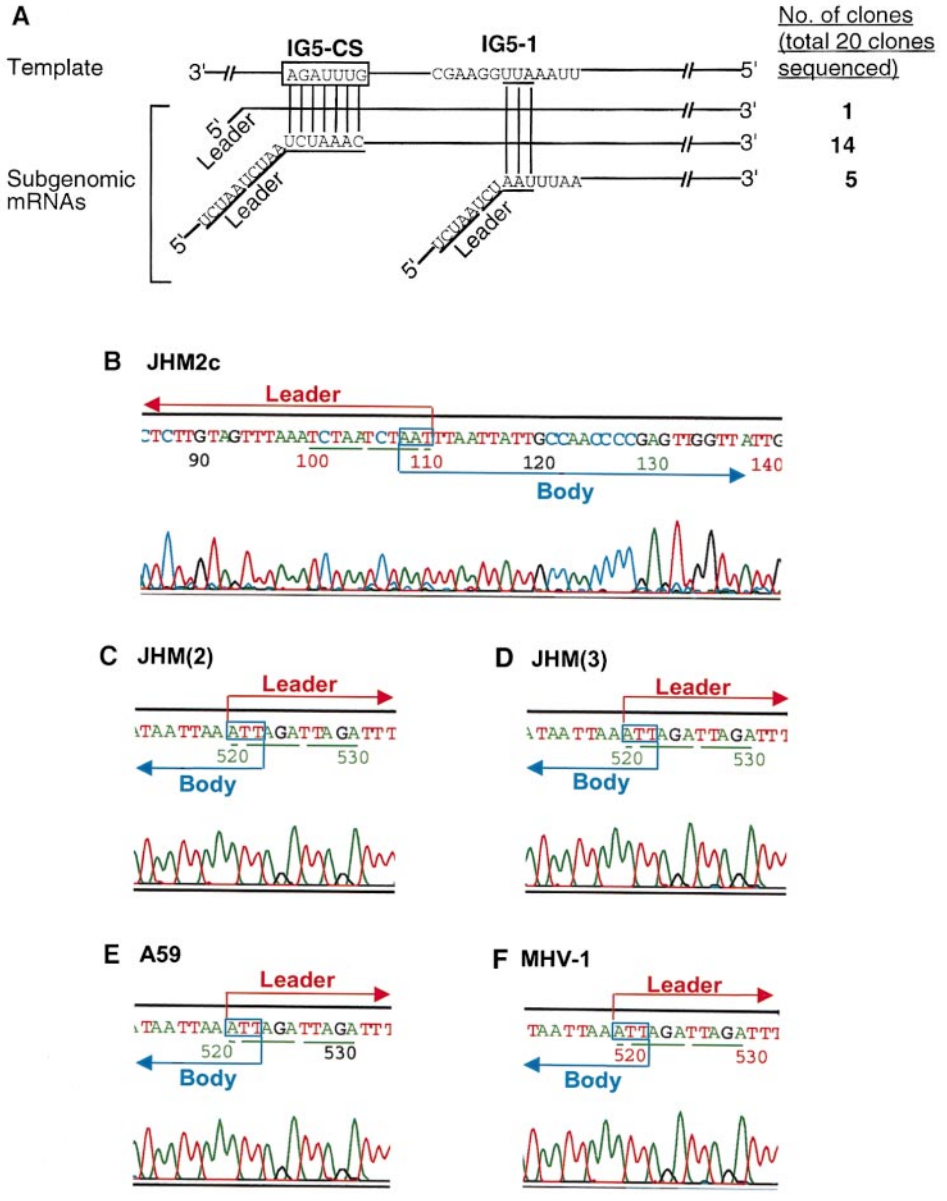

FIG. 2. Summary of the DNA sequencing results. (A) Heterogeneous leader-body fusion sites of JHM2c mRNA5 species revealed by DNA sequencing. Template is shown in (−)-strand. Only the consensus sequence of the intergenic region 5 (IG5-CS) and the transcriptional initiation site for mRNA5–1 (IG5–1) are shown. Vertical lines indicate the complementary sequences at the leader-body fusion site. The number shown on the right to each mRNA species indicates the number of clones, which represent the corresponding mRNA species. A total of 20 clones were sequenced. (B–F), Representative sequencing profiles showing the leader-body fusion site of mRNA5–1 for JHM2c (B), JHM(2) (C), JHM(3) (D), A59 (E), and MHV-1 (F), respectively. DNA sequencing was carried out in the automatic DNA sequencer (ABI Prism Model 377) using the cloned plasmid DNAs with a T7 promoter primer (B) or directly using gel-purified PCR fragments with primer 3′IG6–50 (C–F). The consensus repeat sequence is underlined in green. The leader and mRNA body sequences are indicated with arrows in red and blue, respectively. The three nucleotides (AAT) at the fusion site are boxed in blue.

used as positive and negative controls, respectively. Subgenomic mRNAs were then amplified by RT-PCR with a CAT-specific antisense primer and a leader-specific sense primer. As shown in Fig. 3B, a specific subgenomic mRNA containing the CAT gene was identified in DECAT5–1 RNA- and DECAT7 RNA-transfected cells but not in the mock-transfected cells, indicating that a CAT-containing subgenomic mRNA was specifically transcribed from the 140-nt sequence of DECAT5–1. This result demonstrates that the noncanonical sequence can serve as an initiation signal (promoter) for subgenomic mRNA transcription in a DI RNA-reporter system.

Mutational analysis of the transcriptional initiation signal. To identify the minimal sequence required for subgenomic mRNA transcription, three deletions within the 140-nt sequence were made by PCR, and the deletion fragments were cloned into the DI RNA-CAT reporter vector in place of the wild-type, full-length (140-nt) se-

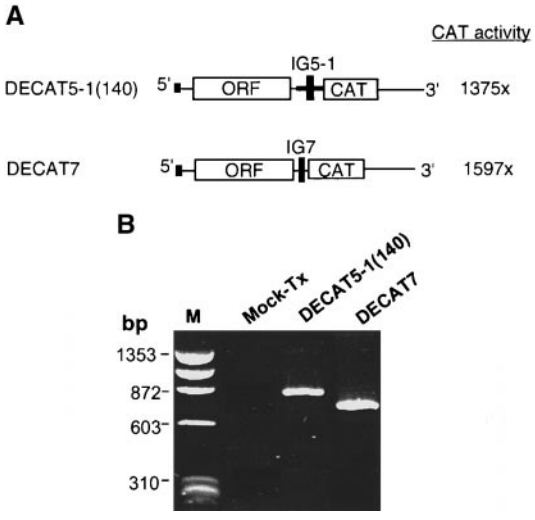

FIG. 3. The noncanonical sequence is a functional promoter for subgenomic mRNA transcription in the defective-interfering (DI) RNA chloramphenicol-acetyltransferase (CAT)-reporter system. (A) The names of the DI RNA CAT reporters are shown on the left and their structures in the middle. CAT activities expressed from these constructs, shown on the right, represent fold-increase against the background, which is set as onefold (1×). The CAT activities are representative of three independent experiments. IG5–1 and IG7 indicate the transcription initiation sites for mRNA5–1 and mRNA7, respectively. ORF, DI open reading frame. (B) Reverse-transcription PCR was performed to detect CAT-containing subgenomic mRNAs using CAT- and leader-specific primers. PCR products were analyzed by electrophoresis on a 1% agarose gel. Lanes Mock-Tx, DECAT5–1(140), and DECAT7 are the RT-PCR products from helper JHM-infected and mock-, DECAT5–1(140) RNA-, and DECAT7 RNA-transfected cells, respectively. M, molecular mass marker in base pair (bp) is shown on the left.

quence (Fig. 4A). The ability of the deleted sequences in initiating subgenomic mRNA transcription was then determined by both the expression of CAT activity and the synthesis of CAT-containing subgenomic mRNAs. As shown in Fig. 4A, when an upstream 63-nt sequence was deleted, the CAT activity was similar to that of the full-length [compare DECAT5–1(140) with DECAT5–1Δ63]. However, when an additional 13-nt sequence was deleted, the CAT activity was significantly reduced to approximately 12-fold above the background (more than 100-fold reduction) [compare DECAT5–1Δ76 with DECAT5–1Δ63 in Fig. 4A). When a construct containing only a 13-nt sequence franking the leader-fusion site was transfected [construct DECAT5–1(13)], 95% of the CAT activity was expressed as compared to the full-length [DECAT5–1(140)], indicating that the 13-nt sequence is sufficient for driving CAT expression. Consistent with the results of CAT activity, subgenomic mRNAs corresponding to the respective constructs were identified by RT-PCR in MHV-infected and DI-transfected cells (Fig. 4B). The noncanonical transcription initiation signal, therefore, contains not more than 13 nt and encompasses the leader-joining site.

To further determine whether this 13-nt core sequence is specifically required for mRNA transcription, three mutations (-GGUUA- to –GGCGC-) were introduced by PCR-based site-directed mutagenesis. When the mutant DI RNA [DECAT5–1(13)m] was transfected, CAT activity expressed from this RNA was drastically decreased (71-fold reduction) (Fig. 4A). No CAT-containing subgenomic mRNA was detectable by RT-PCR (Fig. 4B). These results indicate that the three nucleotides in this core sequence are required for its transcription activity.

Subgenomic mRNA5–1 is a functional message for translation of the E protein in an in vitro *translation system.* To determine whether mRNA 5–1 is a functional message, the open reading frame prediction program of software MacVector (version 3.5) was used to analyze the sequence and to predict the possible ORFs in mRNA5–1. Our analysis indicated that ORF5b is the most probable ORF at the 5′-end of mRNA5–1 (Fig. 5A). To confirm that ORF5b can be expressed from mRNA5–1, a

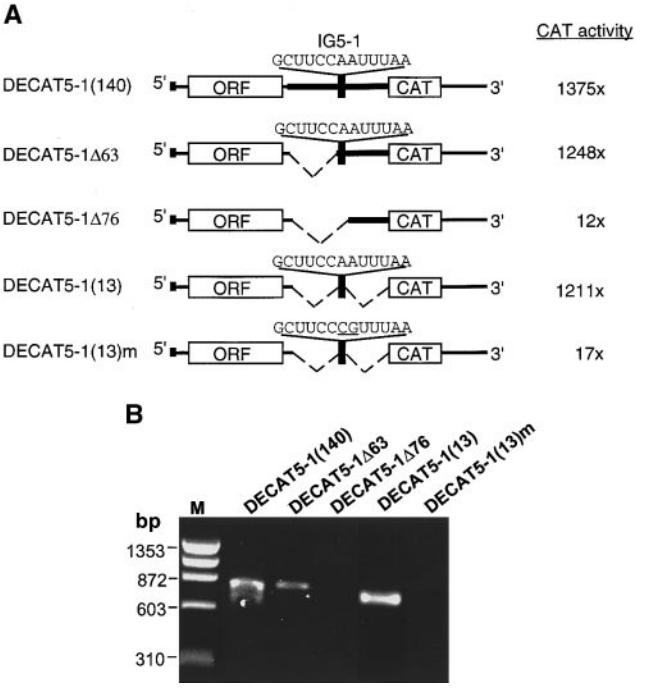

FIG. 4. Deletion mapping of the noncanonical transcription signal. All deletion mutants were made and their transcription activities were examined in the DI-CAT-reporter system. (A) The names of the DI RNA CAT reporters are shown on the left and their structures in the middle. CAT activities expressed from these constructs, shown on the right, represent fold-increase against the background, which is set as onefold (1×). The CAT activities are representative of three independent experiments. IG5–1 indicate the transcription initiation sites for mRNA5–1. Only the 13-nt core sequence of the IG5–1 is shown. ORF, DI open reading frame. Thick lines denote sequence of viral origin, while the thin lines indicate their DI origin. (B) Reverse-transcription PCR was performed to detect CAT-containing subgenomic mRNAs using CAT- and leader-specific primers as described under Materials and Methods. Intracellular RNAs were isolated from MHV-infected and various DI CAT RNA-transfected cells as indicated at the top. PCR products were analyzed by electrophoresis on a 1% agarose gel. M, molecular mass marker in base pair (bp) is shown on the left.

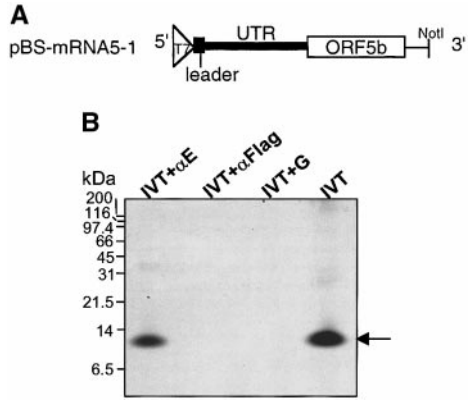

FIG. 5. *In vitro* translation of mRNA5–1. (A) The 5′-end of viral mRNA5–1 was cloned into the plasmid under the control of T7 RNA polymerase promoter (T7). Following restriction enzyme digestion with *Not*I, mRNAs were transcribed *in vitro* with T7 RNA polymerase in the presence of a cap-analog. UTR, untranslated region; ORF5b, open reading frame 5b, which encodes the E protein of MHV. (B) Result of *in vitro* translation. The *in vitro* translation experiment was performed in the rabbit reticulocyte lysate in the presence of ^{35}S-methionine. Ten microliters of *in vitro* translation products were precipitated with an anti-E antibody (lane IVT + αE) or with an unrelated anti-Flag monoclonal antibody (lane IVT + αFlag) or without any antibody (lane IVT + G). Lane IVT represents 10% of the input volume of *in vitro* translation products used for immunoprecipitation. Proteins were analyzed by electrophoresis on 17% SDS–polyacrylamide gel. The arrow indicates the E protein. Prestained protein standard (Bio-Rad) was used as molecular mass marker, which is shown in kilodaltons (kDa) on the left.

cDNA containing the authentic 5′-end of mRNA5–1 (including the leader and ORF5b) was synthesized and cloned into a plasmid vector (Fig. 5A). RNAs were then synthesized by *in vitro* transcription with T7 RNA polymerase. Expression of ORF5b from mRNA5–1 was determined in an *in vitro* translation system. As shown in Fig. 5B, a protein with a molecular mass of approximately 9–12 kDa, which corresponds to the predicted size of ORF5b, the E protein (Yu *et al.,* 1994), was synthesized in the rabbit reticulocyte lysate (lane IVT). This protein was precipitated by an E-specific antibody (lane IVT + αE). The reaction was specific because the same protein could not be precipitated by an unrelated antibody (the M2 monoclonal antibody against the Flag-epitope) (lane IVT + αFlag), or by protein G agarose beads alone (lane IVT + G). These results demonstrate that mRNA5–1 is a functional message and that it translates into the E protein.

Translational regulation of ORF5b in the DI RNA expression system. It was previously reported that the ORF5b of MHV was expressed from the second ORF of mRNA5 via an IRES (Thiel and Siddell, 1994, 1995). Our current data showed that ORF5b could also be expressed from the first ORF of mRNA5–1 in an *in vitro* translation reaction (Fig. 5). An obvious question then is how ORF5b is expressed *in vivo* (in virus-infected cells). To address this question, we made two sets of DI CAT reporter constructs, both of which contain the authentic ORF5a and the CAT gene in place of ORF5b. In the first set, the IG5 consensus sequence and the 5′-UTR are present, so that ORF5a would be expressed from mRNA5, while in the second set the ORF5a would not be expressed due to the absence of mRNA5 transcription (see their structures in Fig. 6). We then transfected these DI RNAs into JHM-infected cells. Detection of the CAT activity would indicate the expression of the ORF5b from these reporter DI RNAs. As expected, high CAT activity was detected in DECAT5-RNA-transfected cells (1384-fold increase over the background) (Fig. 6A). Interestingly, the CAT activity expressed from DECAT5m RNA-transfected cells remained at a high level (921-fold above background level), though it was slightly lower than that of DECAT5. Because there was no subgenomic DI mRNA5–1 transcribed from DECAT5m (Fig. 6B), it is conceivable that the CAT activity must have been expressed

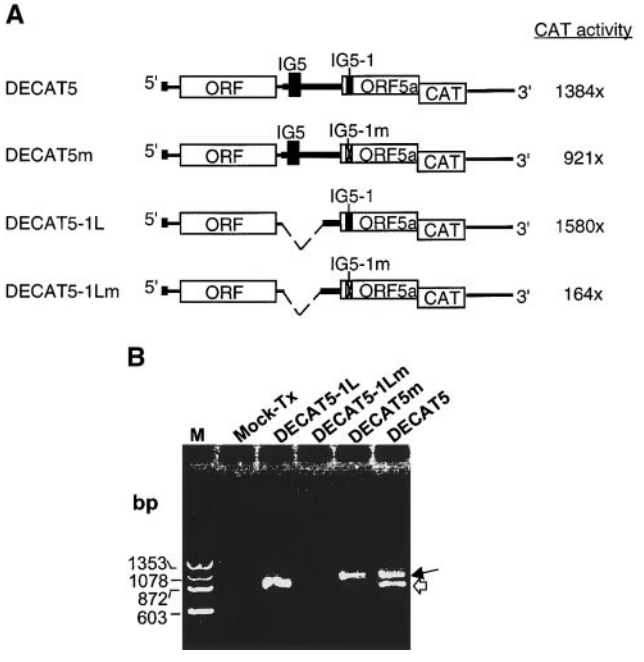

FIG. 6. Analyses of the expression of ORF5b using the defective-interfering (DI) RNA-reporter system. (A) The names of the DI RNA CAT reporters are shown on the left and their structures in the middle. CAT activities expressed from these constructs, shown on the right, represent fold-increase against the background, which is set as onefold (1×). The CAT activities are representative of three independent experiments. IG5 and IG5–1 indicate the transcription initiation sites for mRNA5 and mRNA5–1, respectively. IG5–1m indicates two nucleotide mutations in the IG5–1 sequence. ORF, DI open reading frame. Thick lines denote the sequences derived from the viral genome; dashed lines indicate deletions. (B) Reverse-transcription PCR was performed to detect CAT-containing subgenomic mRNAs using CAT- and leader-specific primers. RNAs were isolated from cells infected with a helper MHV and transfected with various DI CAT RNAs as indicated at the top. Lane Mock-Tx, mock-transfection. PCR products were analyzed by electrophoresis on a 1% agarose gel. The solid arrow denotes PCR products representing mRNAs transcribed from IG5 site, and the unfilled arrow indicates mRNAs transcribed from IG5–1 site. M, molecular mass marker in base pair (bp) is shown on the left.

from either DI mRNA5 or genomic DI RNA, in the latter of which the CAT gene is the third ORF. In both cases, the expression of the CAT activity must be mediated via internal entry of ribosome. When the IG5 consensus sequence was removed and the TIS5–1 was mutated (construct DECAT5–1Lm), the CAT activity was drastically reduced (164-fold above the background). Because neither DI mRNA5 nor DI mRNA5–1 was transcribed from DECAT5–1Lm (Fig. 6B), the low level of CAT activity was likely expressed from the genomic DI RNA via ribosomal internal entry. However, when the wild-type IG5–1 sequence was restored (DECAT5–1L), CAT activity was significantly increased (Fig. 6A). Because the wild-type IG5–1 allowed the transcription of DI mRNA5–1 (Fig. 6B), this result indicates that a large part of the CAT activity was expressed from DI mRNA5–1 (compare the structure and CAT activity of DECAT5–1L with those of DECAT5–1Lm in Fig. 6). Taken together, these results indicate that MHV ORF5b can be expressed from mRNA5, mRNA5–1, and even the genomic RNA *in vivo* using the DI RNA expression system.

DISCUSSION

In this study, we have identified a noncanonical sequence that allows the transcription of a novel subgenomic mRNA species (mRNA5–1) of JHM2c, JHM(2), JHM(3), A59, and MHV-1. Using the MHV DI RNA-CAT reporter system, we were able to demonstrate that the noncanonical sequence serves as a signal for transcription of a subgenomic mRNA (Fig. 3). Although the precise sequence for this transcription signal was not determined, a 13-nt sequence including the leader-joining site was shown to be sufficient for the expression of the DI CAT reporter gene (Fig. 4). Furthermore, the three nucleotides at the leader-joining site appear to be required for its transcription activity, since mutations of these nucleotides abolished subgenomic mRNA transcription (Fig. 4). The computer program MacVector predicts that this novel mRNA species encodes the ORF5b of MHV at its most 5′-end. *In vitro* translation studies with the rabbit reticulocyte lysate confirmed that the E protein is translated from this mRNA (Fig. 5), indicating that this mRNA is a functional transcript. Our results thus establish for the first time that a noncanonical sequence, which has no sequence resemblance to the consensus IG sequence, can serve as a signal for transcription of a functional mRNA in MHV. This finding will have important implications not only in the mechanisms of coronavirus RNA transcription but also in the regulation of coronavirus gene expression both at the transcription and translation levels.

The major feature in coronavirus RNA transcription is the discontinuous process. Regardless of whether the discontinuous transcription occurs during (+)- or (−)-strand synthesis, subgenomic RNA synthesis always involves the interaction between the leader (antileader) and the intergenic sequence. It has been suggested that this interaction is probably mediated by direct RNA–RNA interaction between the complementary sequences (see review by Lai and Cavanagh, 1997, and references therein). Using MHV JHM2c, we previously showed that mRNA2–1 of JHM2c is very heterogeneous at its leader-body joining site (Zhang and Lai, 1994). In addition to those mRNAs whose leader-body fusion occurs at the consensus IG sequence, some mRNAs have a leader fused at either upstream or downstream of the consensus IG sequence. Because these upstream or downstream regions do not have complementary sequences between the leader and the consensus IG site, it is less likely that direct RNA–RNA interaction through complementary sequences is the major determinant for this discontinuous process. While the previous observation reveals a random fashion of the heterogeneous leader-body fusion sites, our present data show a distinct, conserved site, even though both studies have identified noncanonical sequences for leader-body fusion. Thus, our current finding reinforces the notion that direct RNA–RNA base-pairing between the leader (antileader) and the IG region is not the sole mechanism in regulating coronavirus RNA transcription. If base-pairing guides subgenomic RNA transcription as shown in arterivirus (van Marle *et al.,* 1999), then why the remaining consensus sequences that are base-paired with the leader and are distributed throughout the genomes of arteriviruses and coronaviruses do not transcribe subgenomic mRNAs. This fact combined with previous (Zhang and Lai, 1994; Fischer *et al.,* 1997) and current findings further suggests that other mechanisms, i.e., protein–RNA and protein–protein interactions and/or RNA secondary structures (Zhang *et al.,* 1994; Zhang and Lai, 1995; Lai, 1998), are likely involved in this discontinuous transcription process.

With respect to the translation of ORF5b, our data clearly show that, when the ORF was placed at the 5′-most end of an mRNA (pBS-mRNA5–1), it could be translated efficiently both in the rabbit reticulocyte lysate *in vitro* translation system (construct pBS-mRNA5–1 in Fig. 5) and *in vivo* in the DI RNA CAT-reporter system (construct DECAT-5–1L in Fig. 6). These data suggest that ORF5b is possibly expressed from mRNA5–1 via the 5′ cap-dependent mechanism. However, we cannot rule out the possibility of the cap-independent pathway because part of the IRES (Jendrach *et al.,* 1999) is also present in these mRNAs. When the CAT gene was placed in the second ORF of mRNA5 (construct DECAT5m in Fig. 6) or in the third ORF of genomic DI RNA (construct DECAT5–1Lm in Fig. 6), the CAT gene could also be expressed *in vivo* with the DI CAT-reporter system. These results thus clearly indicate that ORF5b can be expressed via internal ribosomal entry, consistent with the finding by Thiel and Siddell (1994, 1995). Jen-

drach *et al.* (1999) reported that the IRES encompassing a region from approximately 100-nt upstream to 180-nt downstream of the ORF5b AUG start codon mediated the translation of ORF5b. Our results showed that the presence of the upstream sequence alone is able to mediate its expression, albeit with low efficiency (Fig. 6). It is important to point out that, although our experimental design was not intended to address the mechanism of translation, the results presented here (Fig. 6) strongly suggest that ORF5b can be expressed from mRNA5, mRNA5–1, and genomic RNA. This finding raises an intriguing question: Why does MHV use multiple pathways to regulate the expression of a single gene? To date, there is no clear answer to this question, but it is known that the expression of the E protein is diverse. For example, the E gene is expressed from the third ORF of mRNA3 in IBV, but from the first ORF of mRNA5–1 of BCoV and of mRNA4 of TGEV and HCoV 229E (Siddell, 1995). Apparently, various coronaviruses have the ability to use different mechanisms for expressing their E protein. Recently, O'Connor and Brian (2000) reported that in TGEV, ORF3b of the Purdue strain is expressed from the first ORF of mRNA3–1, whereas that of the Muller strain is expressed from the second ORF of mRNA3.

Our results offer another interesting possibility that ORF5b may also be expressed from MHV genomic RNA and subgenomic mRNAs 2–4, since they contain the IRES sequence. When the CAT gene was placed as the third ORF in the DI, a low level of CAT activity was expressed (Fig. 6A). One possible explanation is that a low amount of CAT-containing subgenomic DI RNA was transcribed from the mutated IG5–1 site. However, our sensitive RT-PCR could not detect any such mRNA (Fig. 6B). Thus, a more reasonable explanation is that the CAT activity is expressed from the genomic RNA via internal entry of ribosome. This is further supported by the data obtained with the DECAT5m construct. However, by comparing DECAT5–1L with DECAT5–1Lm (Fig. 6), one could conclude that translation of the CAT gene from the genomic DI RNA via internal entry of ribosome must be very inefficient. By analogy to the DI system, our results suggest that the E gene can also be expressed from the genomic RNA and subgenomic mRNAs 2–4, since they all contain the IRES, but that the efficiency of such translation is low. Further investigation on the mechanisms of translation of ORF5b is needed.

It is worth noting that the detection of mRNA5–1 in JHM2c-infected cells is unlikely the result of RT-PCR artifact. We employed the same procedure for amplifying various mRNA species (mRNAs 2–7) and did not identify such conserved mRNA species (Zhang, 2000). By contrast, we were able to amplify mRNA5–1 repeatedly and in an amount proportional to mRNA5 (data not shown). However, mRNA5–1 is a minor species relative to mRNA5 (Figs. 1 and 2). Interestingly, when Makino *et al.* (1984) analyzed the intracellular viral mRNAs of JHM2c and its parental JHM strains, they found that a minor mRNA species (named RNA c) migrated slightly faster than mRNA5 on 1% agarose gel. They noted that it was difficult to separate the major (mRNA5) from the minor (RNA c) RNA species, but possible mixtures were noticeable. Although RNA c was identified in both JHM and JHM2c, it was predominantly present in JHM2c (Makino *et al.,* 1984). Sequence comparison also revealed that the IG5–1 is conserved between JHM and JHM2c (data not shown). Thus, it is tempting to speculate that mRNA5–1 identified in this study might represent RNA c detected by Makino *et al.* (1984). However, RNA c-like mRNA species was not found in A59 and MHV-1. Thus, mRNA5–1 may represent a novel mRNA species.

MATERIALS AND METHODS

Cells, virus, and antibody. The murine astrocytoma cell line DBT (Hirano *et al.,* 1974) was used for virus growth, virus infection, and RNA transfection. The naturally occurring small plaque mutant JHM2c, the parental JHM(2), and JHM(3) strains (Makino *et al.,* 1984, 1988), A59, and MHV-1 were used in this study. The goat antiserum specific to MHV E protein was kindly provided by Dr. Julian Leibowitz, University of Texas in College Station, and its specificity was confirmed previously (Yu *et al.,* 1994). The M2 monoclonal antibody specific to an eight-amino acid flag-epitope was purchased from BAbCo, Inc.

Reverse transcription and polymerase chain reaction and cloning of viral subgenomic mRNAs. For detection of viral subgenomic mRNAs, DBT cells were infected with JHM2c at a multiplicity of infection of 5. Virus grew in the presence of actinomycin D (10 μg/ml). Intracellular RNAs were isolated from cells at 7 h postinfection by the Nonidet P-40 method as described previously (Zhang *et al.,* 1994) and used for cDNA synthesis by RT with an antisense primer 3′IG5–300 (5′-GCG TAG GCC GTG AAG CTA-3′). This primer is complementary to a sequence approximately 300 nucleotides downstream of the IG consensus sequence between genes 6 and 5 of viral RNAs. An additional sense primer (5′L9) specific to the leader (Zhang *et al.,* 1994) was used for the subsequent PCR amplification. The conditions for the RT-PCR were essentially the same as described previously (Zhang and Lai, 1994). Briefly, the RT reaction was carried out at 42°C for 90 min, and the PCR was performed in a thermocycler (DNA Engine PTC-200, M.J. Research) for 30 cycles. The condition for each cycle was denaturation at 95°C for 30 s, annealing at 62°C for 1 min, and extension at 72°C for 1 min. For detection of subgenomic mRNAs containing the CAT reporter gene, RT-PCR was carried out using a CAT-specific antisense primer 3′-CAT542 (5′-TTA CGC CCC GCC CTG CCA CTC ATC GC-3′, complementary to the 3′-end of the CAT ORF) and the leader-specific sense primer 5′-L9. PCR products were analyzed by agarose gel electrophoresis either directly or after cloning and

restriction enzyme digestion as indicated. PCR products were directly cloned into the pTOPO2.1 TA cloning vector (In Vitrogen). For detecting mRNA5–1 in other MHV strains [JHM(2), JHM(3), A59 and MHV-1], the antisense primer 3′-IG6–50 (5′-GCT GTC CAT TGG TAG ACG-3′, complementary to a sequence at nt 30–47 of the ORF6) was used for RT reaction and the primer pair 5′-L9 and 3′-IG6–50 for PCR.

Analysis and sequencing of cDNA clones. All cDNA clones for JHM2c were analyzed by restriction enzyme digestion and agarose gel electrophoresis. RT-PCR products representing cDNA fragments derived from JHM(2), JHM(3), A59, and MHV-1 were purified from agarose gel with the gel extraction kit (GelExII, Qiagen) and used directly for DNA sequencing. Sequences were determined with the automatic DNA sequencer (Model Prizm 377, ABI) in the core facility of the Department of Microbiology and Immunology, UAMS. For sequencing of the cloned DNA, either the T7 promoter primer or the M13 reverse primer was used; for direct sequencing of PCR fragments, primer 3′-IG6–50 was used.

Plasmid constructions. For generating a DI CAT reporter plasmid containing the IG5–1 sequence (upstream of ORF5b), a three-step jumping PCR was performed. In the first PCR, pTA-IG5–370 DNA was used as a template. pTA-IG5–370 contains the 5′-end 370 nt of mRNA5, which was cloned after RT-PCR amplification (see Figs. 1 and 2). The sense primer was 5′-*Spe*IG5–1 (5′-TT*A CTA GT*T GTG AGT GAC GCC T-3′), which contains a *Spe*I site at the 5′-end (italic) and a sequence at nt 81–95 downstream of the consensus IG5 site. The antisense primer was 3′-IG5–1 CAT (5′-*ATT TTT TTC TCC AT*A CCC TGG TTG CTA CA-3′), which contains a sequence from nt 206 to 221 downstream of the consensus IG5 and the first 14 nt of the CAT ORF (italic). In the second PCR, the CAT ORF was amplified from the pDECAT2–1 DNA template (Zhang *et al.,* 1994) with the primer pair 5′-CAT (5′-ATG GAG AAA AAA AT-3′) and 3′CAT542. Products from these two PCR reactions were purified with the Gel Elution Kit (Qiagen) following agarose gel electrophoresis and were used as templates for a third PCR with the primer pair 5′*Spe*IG5–1 and 3′-CAT542. The final PCR products were digested with *Spe*I and *Bsp*EI, and they were directionally cloned into the *Spe*I and *Bsp*EI sites of pDECAT2–1, generating pDECAT5–1(140). This construct contains 140 nt of the IG5–1 sequence in front of the CAT ORF. For making two deletion constructs, pDECAT5–1(140) was used as a template for PCR amplification with the primer pair 5′-*Spe*IG5–1Δ63 and 3′CAT542, and 5′-*Spe*IG5–1Δ76 and 3′CAT542, respectively. 5′-*Spe*IG5–1Δ63 (5′-TT*A CTA GT*G CTT CCA ATT TAA-3′) contains a *Spe*I site (italic) and a sequence at nt 144–156 downstream of the IG5 consensus sequence. 5′-*Spe*IG5–1Δ76 (5′-TT*A CTA GT*T ATT GCC AAC CCC GA-3′) contain a *Spe*I site at the 5′-end (italic), and a sequence at nt 157–172 downstream of IG5 consensus sequence. The PCR products were digested with *Spe*I and *Bsp*EI, and directionally cloned into the *Spe*I and *Bsp*EI sites of pDECAT2–1, resulting in pDECAT5–1Δ63 and pDECAT5–1Δ76, respectively (Fig. 4). For creating DI CAT reporter constructs containing the 13-nt core sequence and its mutant, DNAs were synthesized from the pDECAT2–1 DNA templates by PCR with the primer pairs 5′-*Spe*IG5–1(13)CAT (5′-TT*A CTA GT***G CTT CCA ATT TAA** ATG GAG AAA AAA AT-3′) and 3′-CAT542, and 5′-*Spe*IG5–1(13)CGC-CAT (5′-TT*A CTA GT***G CTT CCC GCT TAA** ATG GAG AAA AAA AT-3′) and 3′-CAT542, respectively. Both 5′-primers contain a *Spe*I site at the 5′-end (italic) and the first 14 nucleotides of the CAT ORF at the 3′-end. While 5′-*Spe*IG5–1(13)CAT contains the wild-type, core 13-nt sequence downstream of the IG5 consensus sequence, 5′-*Spe*IG5–1(13)CGC-CAT has 3-nt mutations within this core sequence (double-underlined). PCR fragments were digested with *Spe*I and *Bsp*EI and directionally cloned into pDECAT2–1, resulting in pDECAT5–1(13) and pDECAT5–1(13)m, respectively (Fig. 4).

To construct pDECAT5 (Fig. 6), RT-PCR was performed to generate cDNA fragments encoding the 5a gene from JHM2c RNA with the sense primer 5′-IG5–70 (5′-GTC TAC CTT GGT AGT TCA A-3′, corresponding to nt 70 to 53 upstream of the IG5 consensus sequence) and the antisense primer 3′-IG5abCAT [5′-*ATT TTT TTC TCC AT*T AAA TTA AAC ATT TC-3′, complementary to the first 14 nt of CAT ORF (italic) and a sequence at the overlapping junction between JHM2c ORF 5a and 5b]. In the second PCR, the CAT ORF was synthesized with primers 5′-CAT and 3′-CAT542. PCR products were purified with the Gel Elution Kit (Qiagen) following agarose gel electrophoresis and used as templates for a third PCR with the primer pair 5′-IG5–70 and 3′-CAT542. The PCR products were digested with *Spe*I (a natural *Spe*I site present immediately upstream of the IG5 consensus sequence) and *Bsp*EI, and the digested fragments were directionally cloned into the *Spe*I and *Bsp*EI sites of pDECAT2–1, generating pDECAT5. To create mutant pDECAT5m (Fig. 6), an upstream DNA fragment was amplified from pDECAT5 DNA templates with the sense primer 5′-IG5–70 and an antisense primer 3′-IG5bMCG [5′-AAC GGG AAG CAA AAA TCT-3′, complementary to a sequence at the IG5–1 site with 2-nt mutations (double-underlined)]. An overlapping downstream DNA fragment was amplified from the same templates with the sense primer 5′-IG5bMCG [5′-UUU UGC UUC CCG UUU AAU UAU UGC CA-3′, corresponding to a sequence at IG5–1 site with 2-nt mutations (double-underlined)] and the antisense primer 3′-CAT542. These two PCR fragments were purified and used as templates for the third PCR, in which the primer pair 5′-IG5–70 and 3′-CAT542 was used. Products were cloned into the pDECAT2–1 in the same manner as for pDECAT5. For constructing pDECAT5–1L and pDECAT5–1Lm, PCR was performed with the pair of primers (5′-*Spe*IG5–1 and 3′-CAT542) on

the template DNAs of pDECAT5 and pDECAT5m, respectively. The PCR products were digested with *Spe*I and *Bsp*EI and directionally cloned into the pDECAT2–1. Mutations of these clones were confirmed by DNA sequencing.

For *in vitro* transcription and translation study, a plasmid containing the 5′-end authentic mRNA5–1 sequence was constructed in three steps. First, a cDNA was synthesized with RT-PCR with the sense primer 5′*Spe*IG5–1 and the antisense primer 3′IG6–50. PCR products were digested with *Dra*I to remove the 5′-end sequence of ≈115 nt. Second, PCR was performed to generate a cDNA containing the 5′-end of mRNA5–1 using pTA-mRNA5–1 DNA as a template, which was cloned in the pTOPO2.1 TA vector (see Figs. 1 and 2). The primer pair was T7 promoter primer and 3′IG5–300. Third, DNA fragments from the first and second PCR were mixed and used as templates for a third PCR, in which the primer pair (the sense T7 promoter primer and the antisense primer 3′IG6–50) was used. PCR fragments were digested with *Sna*BI and blunt-ended with T4 DNA polymerase and used for cloning. pDECAT2–1 DNA was digested with *Sna*BI and *Xba*I to remove all but the 5′-end 24-nt of the DI RNA, blunt-ended, and used as a vector for cloning of the above PCR fragments. The resultant plasmid pBS-mRNA5–1 contains the 5′-end of mRNA5–1 with the complete ORF5b (Fig. 5).

In vitro transcription and RNA transfection. For generating DI RNA for transfection, plasmid DNAs were linearized with *Xba*I. RNAs were transcribed with T7 RNA polymerase using the MegaScript *in vitro* transcription kit according the manufacturer's instruction (Ambion). For generating mRNAs for *in vitro* translation study, plasmid DNAs were linearized with *Xba*I. Capped mRNAs were transcribed with the MegaScript kit in the presence of cap-analog (BRL-Gibco). DNA templates were digested with RQ DNase I (Promega). mRNAs were purified with G25 column (Ambion). The *in vitro* transcribed DI RNAs were transfected into MHV-infected DBT cells with the transfection reagent DOTAP according to the manufacturer's instruction (Boehringer Mannheim) as described previously (Zhang and Lai, 1994).

Extraction of cell lysate and CAT assay. Infected and transfected DBT cells from a 60-mm Petri dish were harvested at 8 h p.i. in most experiments, resuspended in 150 μl of 0.25 M Tris–HCl (pH 8.0), and lysed by freezing and thawing three times. Cellular lysate was incubated at 60°C for 10 min. Following a brief centrifugation, 50 μl of each sample was assayed for CAT activity using an assay kit according to the manufacturer's instructions (Promega). The CAT reaction was carried out for 12 h as described previously (Zhang *et al.,* 1994).

In vitro translation. The *in vitro* translation reaction was carried out in the nuclease-treated rabbit reticulocyte lysate system in the presence of ^{35}S-methionine using the *in vitro* transcribed RNAs according to the manufacturer's recommendations (Promega).

Immunoprecipitation. Immunoprecipitation was carried out in 200 μl of radioimmunoprecipitation assay (RIPA) buffer (50 mM Tris, pH 7.4, 150 mM NaCl, 0.5% NP-40, 0.1% SDS, 1 mM PMSF) containing 10 μl of the *in vitro* translation products and 1 μl of the goat-anti-E polyclonal antiserum by constant rocking on a rocking platform at 4°C overnight. The antibody-antigen complexes were then precipitated with protein G-agarose beads (Boehringer Mannheim) at 4°C for 2 h. Agarose beads were washed 3–5 times with RIPA buffer. Protein complexes were denatured by boiling for 3 min in Lammeli's sample loading buffer (100 mM Tris, pH 6.8, 200 mM DTT, 4% SDS, 0.2% bromphenal blue, 20% glycerol) and analyzed by SDS-polyacrylamide gel electrophoresis. The gels were exposed to X-ray film and autoradiographed.

ACKNOWLEDGMENTS

This work was supported by the United States Public Health Services Grants AI 41515 and AI 47188 from the National Institutes of Health (to X.M.Z.). We thank Dr. Julian Leibowitz for kindly providing the anti-E protein antiserum.

REFERENCES

Budzilowicz, C. J., Wilczynski, S. P., and Weiss, S. R. (1985). Three intergenic regions of coronavirus mouse hepatitis virus strain A59 genome RNA contain a common nucleotide sequence that is homologous to the 3′-end of the viral mRNA leader sequence. *J. Virol.* **53,** 834–840.

Fischer, F., Stegen, C. F., Koetzner, C. A., and Masters, P. S. (1997). Analysis of a recombinant mouse hepatitis virus expressing a foreign gene reveals a novel aspect of coronavirus transcription. *J. Virol.* **71,** 5148–5160.

Godet, M., Haridon, R., Vautherot, J. F., and Laude, H. (1992). TGEV coronavirus ORF4 encodes a membrane protein that is incorporated into virions. *Virology* **188,** 666–675.

Hirano, N., Fujiwara, K., Hino, S., and Matsumoto, M. (1974). Replication and plaque formation of mouse hepatitis virus (MHV-2) in mouse cell line DBT culture. *Arch. Gesamte Virusforsch.* **44,** 298–302.

Jendrach, M., Thiel, V., and Siddell, S. G. (1999). Characterization of an internal ribosome entry site within mRNA5 of murine hepatitis virus. *Arch. Virol.* **144,** 921–933.

Lai, M. M. C. (1998). Cellular factors in the transcription and replication of viral RNA genomes: a parallel to DNA-dependent RNA transcription. *Virology* **244,** 1–12.

Lai, M. M. C., Baric, R. S., Brayton, P. R., and Stohlman, S. A. (1984). Characterization of leader RNA sequences on the virion and mRNAs of mouse hepatitis virus-a cytoplasmic RNA virus. *Proc. Natl. Acad. Sci. USA* **81,** 3626–3630.

Lai, M. M. C., and Cavanagh, D. (1997). The molecular biology of coronaviruses. *Adv. Virus Res.* **48,** 1–100.

Lai, M. M. C., Brayton, P. R., Armen, R. C., Patton, C. D., Pugh, C., and Stohlman, S. A. (1981). Mouse hepatitis virus A59: Messenger RNA structure and genetic localization of the sequence divergence from the hepatotropic strain MHV 3. *J. Virol.* **39,** 823–834.

Lai, M. M. C., Patton, C. D., Baric, R. S., and Stohlman, S. A. (1983). The presence of leader sequences in the mRNA of mouse hepatitis virus. *J. Virol.* **46,** 1027–1033.

Lee, H. J., Shieh, C. K., Gorbalenya, A. E., Koonin, E. V., La Monica, N.,

Tuler, J., Bagdzyahdzhyan, A., and Lai, M. M. C. (1991). The complete sequence (22 kilobases) of murine coronavirus gene 1 encoding the putative proteases and RNA polymerase. *Virology* **180,** 567–582.

Leibowitz, J. L., Wilhemsen, K. C., and Bond, C. W. (1981). The virus-specific intracellular RNA species of two murine coronaviruses: MHV-A59 and MHV-JHM. *Virology* **114,** 39–51.

Liao, C. L., and Lai, M. M. C. (1994). Requirement of the 5′-end genomic sequence as an upstream *cis*-acting element for coronavirus subgenomic mRNA transcription. *J. Virol.* **68,** 4727–4737.

Liao, C.-L., Zhang, X. M., and Lai, M. M. C. (1995). Coronavirus defective-interfering RNA as an expression vector: the generation of a pseudorecombinant mouse hepatitis virus expressing hemagglutinin-esterase. *Virology* **208,** 319–327.

Makino, S., and Lai, M. M. C. (1989a). Evolution of the 5′-end of genomic RNA of murine coronaviruses during passages in vitro. *Virology* **169,** 227–232.

Makino, S., and Lai, M. M. C. (1989b). High-frequency leader sequence switching during coronavirus defective interfering RNA replication. *J. Virol.* **63,** 5285–5292.

Makino, S., Joo, M., and Makino, J. K. (1991). A system for study of coronavirus mRNA synthesis: A regulated expressed subgenomic defective interfering RNA results from intergenic site insertion. *J. Virol.* **65,** 6031–6041.

Makino, S., Soe, L. H., Shieh, C. K., and Lai, M. M. C. (1988). Discontinuous transcription generates heterogeneity at the leader fusion sites of coronavirus mRNAs. *J. Virol.* **62,** 3870–3873.

Makino, S., Taguchi, F., Hirano, N., and Fujiwara, K. (1984). Analysis of genomic and intercellular viral RNAs of small plaque mutants of mouse hepatitis virus, JHM strain. *Virology* **39,** 138–151.

O'Connor, J. B., and Brian, D. A. (2000). Downstream ribosomal entry for translation of coronavirus TGEV gene 3b. *Virology* **269,** 172–182.

Pachuk, C. J., Bredenbeek, P. J., Zoltick, P. W., Spaan, W. J. M., and Weiss, S. R. (1989). Molecular cloning of the gene encoding the putative polymerase of mouse hepatitis coronavirus strain A59. *Virology* **171,** 141–148.

Schaad, M. C., and Baric, R. S. (1993). Evidence for new transcriptional units encoded at the 3′ end of the mouse hepatitis virus genome. *Virology* **196,** 190–198.

Shieh, C. K., Lee, H. J., Yokomori, K., La Monica, N., Makino, S., and Lai, M. M. C. (1989). Identification of a new transcriptional initiation site and the corresponding functional gene 2b in the murine coronavirus RNA genome. *J. Virol.* **63,** 3729–3736.

Siddell, S. G. (1995). The small membrane protein. In *The Coronaviridae* (S. G. Siddell, Ed.), pp. 181–190. Plenum, New York.

Smith, A. R., Boursnell, M. E., Binns, M. M., Brown, T. D., and Inglis, S. C. (1990). Identification of a new membrane-associated polypeptide specified by the coronavirus infectious bronchitis virus. *J. Gen. Virol.* **71,** 3–11.

Spaan, W. J. M., Delius, H., Skinner, M., Armstrong, J., Rottier, P., Smeekens, S., van der Zeijst, B. A. M., and Siddell, S. G. (1983). Coronavirus mRNA synthesis involves fusion of non-contiguous sequences. *EMBO J.* **2,** 1839–1844.

Thiel, V., and Siddell, S. G. (1994). Internal ribosome entry in the coding region of murine hepatitis virus mRNA5. *J. Gen. Virol.* **75,** 3041–3046.

Thiel, V., and Siddell, S. G. (1995). Translation of the MHV sM protein is mediated by the internal entry of ribosomes on mRNA5. In *Corona- and Related Viruses* (P. J. Talbot and G. A. Levy, Eds.), pp. 311–315. Plenum, New York.

van Marle, G., Dobbe, J. C., Gultyaev, A. P., Luytjes, W., Spaan, W. J. M., and Snijder, E. J. (1999). Arterivirus discontinuous mRNA transcription is guided by base pairing between sense and antisense transcription-regulating sequences. *Proc. Natl. Acad. Sci. USA* **96,** 12056–12061.

Vennema, H., Godeke, G. J., Rossen, J. W. A., Voorhout, W. F., Horzinek, M. C., Opstelten, D. J. E., and Rottier, P. J. M. (1996). Nucleocapsid-independent assembly of coronavirus-like particles by co-expression of viral envelope protein genes. *EMBO J.* **15,** 2020–2028.

Yu, X., Bi, W., Weiss, S. R., and Leibowitz, J. L. (1994). Mouse hepatitis virus gene 5b protein is a new virion envelope protein. *Virology* **202,** 1018–1023.

Zhang, X. M. (2000). Heterogeneity of subgenomic mRNAs of a mutant mouse hepatitis virus strain JHM2c. In *The Nidoviruses* (E. Lavi *et al.*, Eds.), Plenum, New York.

Zhang, X. M., and Lai, M. M. C. (1994). Unusual heterogeneity of leader-mRNA fusion in a murine coronavirus: Implications for the mechanism of RNA transcription and recombination. *J. Virol.* **68,** 6626–6633.

Zhang, X. M., and Lai, M. M. C. (1995). Interaction between the cytoplasmic proteins and the intergenic (promoter) sequence of mouse hepatitis virus RNA: Correlation with amount of subgenomic mRNA transcribed. *J. Virol.* **69,** 1637–1644.

Zhang, X. M., Liao, C. L., and Lai., M. M. C. (1994). Coronavirus leader RNA regulates and initiates subgenomic mRNA transcription both in trans and in cis. *J. Virol.* **68,** 4738–4746.

Zhang, X. M., Hinton, D. R., Cue, D., Stohlman, S. A., and Lai, M. M. C. (1997). Expression of gamma interferon by a coronavirus defective-interfering RNA vector and its effect on viral replication, spread and pathogenicity. *Virology* **233,** 327–338.

Zhang, X. M., Hinton, D. R., Parra, B., Park, S., Liao, C. L., Lai, M. M. C., and Stohlman, S. A. (1998). Expression of hemagglutinin/esterase by a mouse hepatitis virus coronavirus defective-interfering RNA alters viral pathogenesis. *Virology* **242,** 170–183.